Protein Dynamics and EPR-spectroscopy: Comparison of Molecular Dynamic Simulations with Experiments

Heinz-Jürgen Steinhoff and Christine Karim

Institut für Biophysik, Ruhr-Universität Bochum, Universitätsstraße 150, 4630 Bochum, F.R.G.

Biophysical Chemistry / Computer Experiments / Molecular Dynamics / Spectroscopy, Electron Spin Resonance

Electron paramagnetic resonance (EPR) experiments and molecular dynamics simulations on the residual motion of hemoglobin bound spin labels provide information about dynamical and rate processes in proteins. Rapid (ps time range) reorientational fluctuations of the nitroxide ring of the spin labels within a conformational substate can be experimentally characterized and distinguished from low frequency (ns time range) transitions between the conformational substates which are observed above 200K in solved samples. A comparison of the experimentally determined magnitudes and frequencies of the reorientational motions and the results of molecular dynamics simulations for several nitroxide localizations yields good agreement for the short time dynamics. Evidence for relatively large scale motions involving rare jumps are observed in the molecular dynamics trajectories. A simple approach using Kramers' theory and a two state jump model permits to combine EPR results and molecular dynamics simulations in the case of these rare events.

1. Introduction

Experiments [1,2] and computer simulations [3] show that a protein can assume a large number of slightly different structures, called conformational substates. At physiological temperatures a protein fluctuates rapidly from substate to substate and these motions are crucial for its function. Proteins are complex systems and the investigation even of simple proteins when extended into previously unexplored regions of time or temperature or when performed with new techniques reveals novel features [4]. Here we study fluctuations and rate processes in hemoglobin using electron paramagnetic resonance (EPR) spectroscopy in combination with molecular dynamics (MD) simulations. The comparison of the results of both methods may be understood as a test of MD simulations against EPR measurements. Beyond that the combination of both methods will enhance the interpretation of EPR spectra and the understanding of fluctuation and rate processes in proteins and systems of similar complexity.

EPR spectroscopy of spin labelled biomolecules, where a stable nitroxide free radical (spin label) is attached at a specific site, has been a highly successful technique which gives insight into the structure and dynamics of proteins [5–7]. Using this technique dynamic processes occuring in proteins may be extracted in several ways. The incomplete averaging of the anisotropic interaction of the electron spin with the nitrogen nuclear spin and the magnetic field gives rise to spectral lineshapes that indicate the reorientational rate and amplitude of the nitroxide fluctuations over correlation times ranging from 10^{-11} to 10^{-6} s. If the rotational diffusion of the whole protein is restricted by crystallization or by solvents of high viscosity the detected motion of a surface nitroxide side chain is that relative to the protein while that for a buried nitroxide side chain reflects local protein structure fluctuation. Typical fluctuation rates and amplitudes and the dependence on hydration and solvent viscosity have been determined for nitroxide side chains attached to hemoglobin for these two types of nitroxide localizations [8,9]. Collision rates between nitroxides bound to adjacent sites at the surface of lysozyme have been determined through Heisenberg exchange rates and through the modulation of the dipole-dipole interaction and their influences on spectral parameters and longitudinal relaxation times T_1 [10].

The dynamics of proteins can also be studied using theoretical methods. In molecular dynamics (MD) simulations, Newtonian equations of motion for the atoms of the protein and any surrounding solvent are solved for the atomic positions as a function of time. With currently available computers it is possible to simulate the dynamics of small proteins for up to a few hundred picoseconds. Such periodes are long enough to characterize completely the librations of small groups in the protein and to determine the dominant contibutions to the atomic fluctuations [11,12].

In the past comparisons between the rms magnitude of the fluctuations of the individual atoms of several proteins calculated from MD simulations and the values of the temperature factors derived from X-ray spectra have been made [13–15]. Furthermore the simulations provide informations about the time variations of structural parameters such as torsion angles and interatomic distances. These parameters may be determined by nuclear magnetic resonance (NMR) measurements and comparisons of MD and NMR results have been performed [16,17]. The aim in the present paper is to compare EPR experiments which are determined by the dynamics of nitroxide side chains on the pico second time scale with molecular dynamics simulations that last up to 135 ps. We make contact between molecular dynamics simulations of spin labelled hemoglobin in vacuo and with

  0005-9021/93/0202-0163 $ 10.00+.25/0

the spin label binding site covered with water and EPR studies of the lyophylized dry and solved molecules by comparing the magnitude of the reorientational fluctuations of the bound spin labels extracted from the experimental data with those calculated from the simulated trajectories. The main fluctuations observed in the ps time range appear to be dominated by a harmonic torsional oscillation of the nitroxide ring. Additionally large scale fluctuations involving rare jumps between different potential wells (conformational substates) are observed and we make an attempt to bridge the short time dynamics and experimentally observed fluctations in the ns time range using a two state jump model.

2. Molecular Dynamics Simulation Procedure

2.1. Model Systems and Data Evaluation

The molecular dynamics simulations are performed on an IRIS 4D25 (Silicon Graphics) using INSIGHT and DISCOVER (Biosym). The atomic coordinates of the αβ dimer of horse methemoglobin (methb) are taken from the Brookhaven Protein Data Bank [18]. The spin label N-(1-oxyl-2,2,6,6-tetramethyl-4-piperidinyl)iodoacetamide (JaaSl) is built according to the data given by Lajzerowicz-Bonneteau [19]. The modification of the hemoglobin molecule with the spin labels at the cystein β93 is done with the help of stereo drawings of the spin labelled binding site determined by Moffat [20] by means of X-ray difference Fourier techniques. The modified molecules are energy minimized with the conjugate gradient procedure to reduce unfavorable interactions resulting from overlap of nonbonded atoms. The detailed molecular dynamics to be analyzed is determined by the molecular dynamics simulation in which the classical equations of motion are investigated. The time step of integration is 1 fs. Atomic velocities are continuously relaxed towards a Maxwell distribution for the first 100 steps according to a temperature of 10K. This step is repeated several times with new velocity assignments corresponding to successively increasing temperatures up to 300K. After this equilibration periode the actual simulation is carried out.

We performed simulations of the following four model systems:

1. The whole methemoglobin tetramer with two spin labels of fixed orientation which displace the side chains of Tyr HC2(β145) of the respective β-subunit. This orientation is identified by Moffat with the strongly immobilized label orientation A originally described by McConnell and Hamilton [21]. In this conformation the nitroxide ring of the label is burried inside the tyrosin pocket. The length of the trajectory is 15 ps.

2. One β-subunit with a spin label of unhindered orientation on the surface of the molecule. This structure will be marked B according to the works of Moffat and McConnell et al. [20,21]. The length of the trajectory of this conformation is 10 ps.

3. A segment of the modified β-subunit with the label position B. This segment contains 19 amino acids including the spin label with 340 atoms (β87−β100, β142−β146, JaaSl). To conserve the structure at the intersection 165 atoms are fixed. The length of the trajectory is 100 ps.

4. The same protein segment as described under point 3) covered with 743 water molecules. The integration of the equations of motion are performed with periodic boundary conditions and the length of the trajectory obtained is 135 ps.

The direct results of a dynamic simulation are the coordinates and velocities of all atoms as a function of time. In the present analysis of the data we restrict ourselves to the coordinates of the nitroxide spin label bound to the hemoglobin molecule. The molecular y and z axes of the spin label are taken parallel to the C−C direction and perpendicular to the C−N−C plane of the nitroxide group, respectively. The molecular x axis coincides with the perpendicular to axes y and z. The presentation of the simulated data in the remainder of the paper will be in a coordinate system $X'Y'Z'$ which is defined by a time average of the nitroxide molecular axes directions x, y, z. Reorientations of the nitroxide ring are parameterized by the angles Φ_1, Φ_2, and Φ_3 about the three axes X', Y' and Z' respectively. To compare the simulated data with results determined from EPR experiments it is useful to define additionally the conventional angles in spherical coordinates, θ and φ as shown in Fig. 1, which characterize the temporary orientation of the nitroxide molecular axis $z(t)$ with respect to the system $X'Y'Z'$.

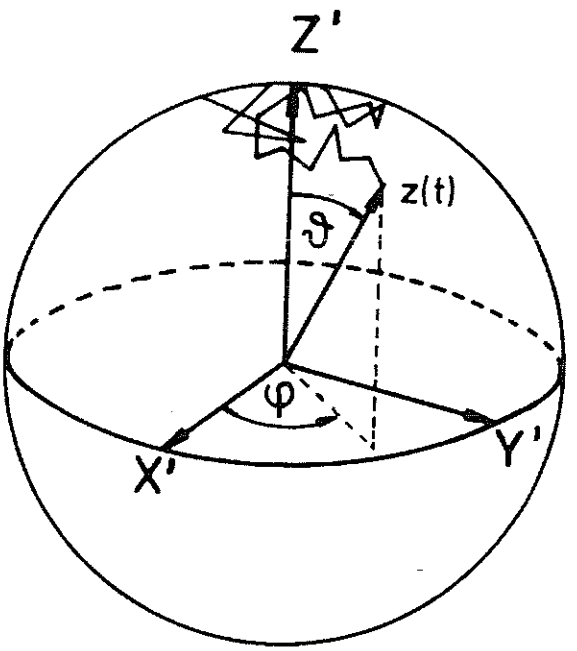

Fig. 1
Illustration of wobble of the nitroxide molecular $z(t)$ axis within the coordinate system $X'Y'Z'$

A part of the $\Phi_1(t)$ trajectory obtained for model systems 3 and 4 are shown in Fig. 2, which illustrates two major types of fluctuations. On a short time scale (1 ps) angle fluctuations with rms amplitudes of 10°−15° are found, and these represent motions within a single potential well. On a

longer time scale (10ps or greater) there occur rare events involving large changes of the angle Φ. These represent jumps between different potential wells. So these fluctuations are involved with transitions between different conformational substates. Similar behavior is observed in the Φ_i trajectories obtained with the other model systems: one of the nitroxide rings of the two labels attached to the methemoglobin tetramer changes its average orientation by an amount of more than 30° for Φ_1 and Φ_2 after the first 11ps of simulation. This behavior is in agreement with the results for interproton dihedral angle fluctuations reported for BPTI and torsion angle fluctuations for the Met-105 side chain of lysozyme [17]. We cannot make any statistics from our relatively short simulations concerning these rare events. Nevertheless, we will show in the experimental section of the paper that these jumps may be attributed to low frequency transitions which are experimentally observed for temperatures above 200K.

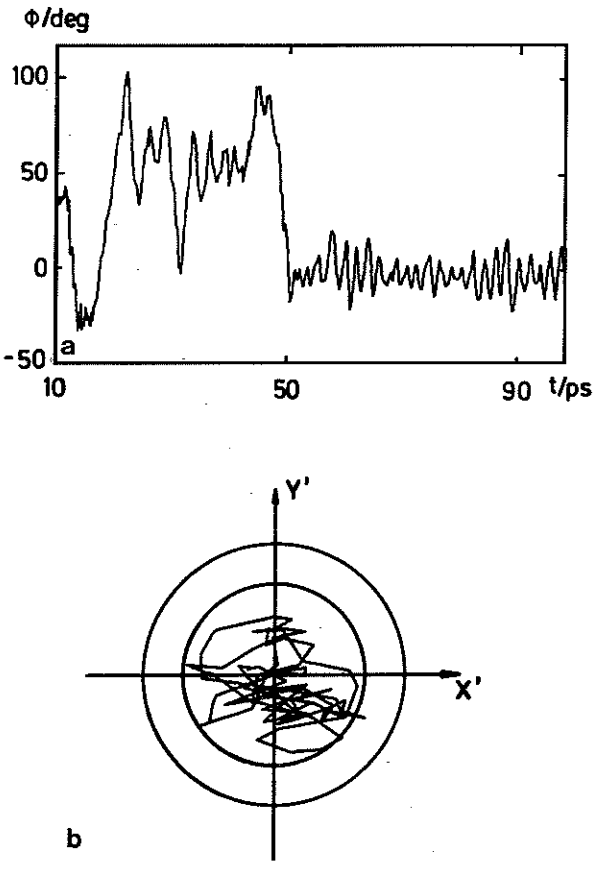

Fig. 2
a) Part of the Φ_1 trajectory, i.e. the reorientation of the nitroxide ring about the X' axis, obtained for model system 3.
b) Projection of the nitroxide molecular $z(t)$ axis onto the $X'-Y'$-plane determined from the last 5 ps of the trajectory of model system 4. The circles are lines of constant θ, $\theta = 20°$ and 30°, respectively

For the stochastic analysis of the Φ_i motion within a conformational substate we select parts of the trajectories which are free from transitions, e.g. the trajectory part beginning at $t=50$ps shown in Fig.2a. The projection of the endpoint of the vector $z(t)$ of system 4 for the last five pico seconds onto the $X'Y'$-plane shows the nearly isotropic fluctuation of this vector with respect to the angle φ (see Fig.2b). A frequency analysis of this motion is made and magnitudes of the angle fluctuations are calculated.

Fig.3 shows the spectral densities $J_{\Phi_1}(\omega)$ for the four model systems, determined from the Fourier transform of the trajectories

$$J_{\Phi_1}(\omega) = 2/T \left| \int_0^T e^{-i\omega t}\, \Phi_1(t)\, dt \right|^2 \tag{1}$$

where T is the total time of the respective trajectory. The angular spectral densities are dominated by swinging motions of the nitroxide ring. The central frequency of this motion is between $0.4 \cdot 10^{12}$ s^{-1} and $0.7 \cdot 10^{12}$ s^{-1} for the vacuum simulations and is shifted to higher values for the molecule segment covered with water. This behavior is due to the coupling of the label motion to the water fluctuations and is consistent with the results given by Brooks and Karplus [22] and Ahlström et al. [23]. Ahlström and coworkers found a shortening of the correlation times for the reorientation of polar amino acids having contact to the solvent going from the vacuum to the water covered system. The damping of the observed oscillating reorientations, which is reflected by the width of the spectral density peak, is lowest for the model system consisting of the protein segment in vacuum (3) and largest for the segment covered with water. This behavior reflects the increasing coupling of the spin label to intramolecular and intermolecular fluctuating forces through van-der-Waals contacts for systems 1, 2 and 4.

2.2. The Model of a Brownian Oscillator

One possible approach to investigate this coupling qualitatively is to apply Brownian motion theory of a particle in a harmonic potential and in contact with a heat bath. Within this theory the variable angle $\chi(t)$ is treated as a stochastic variable obeying the Langevin equation

$$\ddot{\chi}(t)+\omega_1^2\chi(t)+\beta_1\dot{\chi}(t) = A(t) \tag{2}$$

where the stochastic influences have been partitioned into a damping term, $\beta\dot{\chi}(t)$, and a remaining stochastic force, $A(t)$. The ensemble average and autocorrelation function of $A(t)$ are given by

$$\langle A(t)\rangle = 0 \tag{3}$$

and

$$\langle A(t)\, A(t+\tau)\rangle = 2\beta kT\, \delta(\tau)/I \tag{4}$$

respectively, where $\delta(\tau)$ is a Dirac delta function, kT the product of the Boltzmann constant and temperature and I is the moment of inertia. The autocorrelation function of

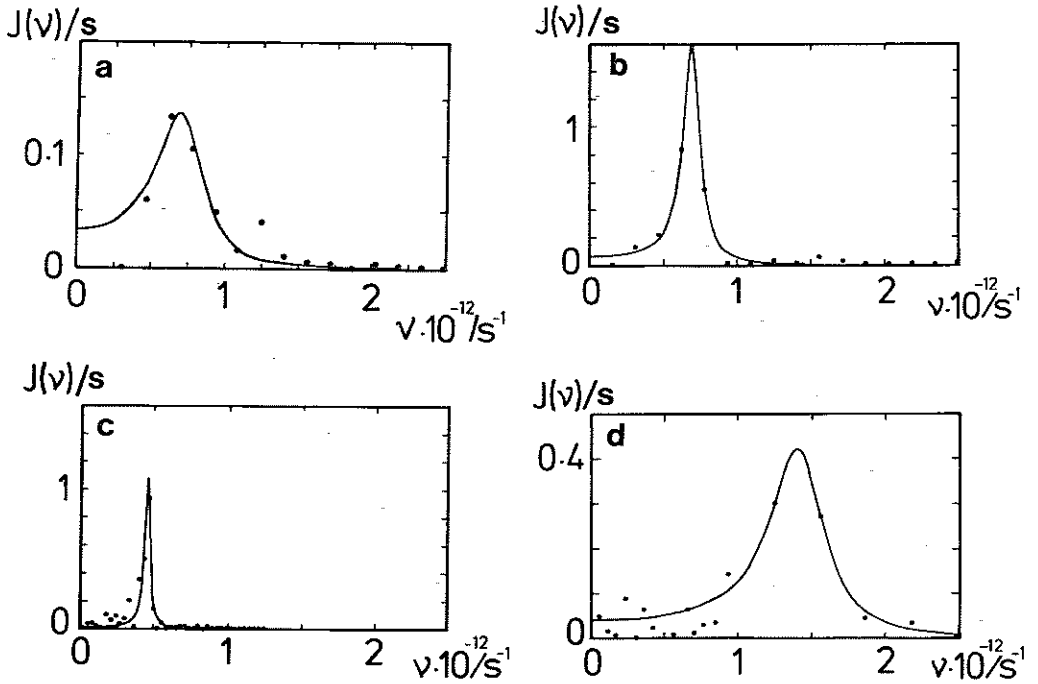

Fig. 3
Spectral densities $J(\nu = \omega/2\pi)$ determined for the fluctuations of Φ_i for different model systems (●) and fitted curves according to Eq.(7): a) model system 1; b) model system 2; c) model system 3 and d) model system 4

$\chi(t)$ can be obtained analytically from the solution of Eq.(2) [24]

$$\langle \chi(t)\,\chi(t+\tau)\rangle = \langle \chi^2(t)\rangle\, e^{-\beta_1\tau/2} \cdot \{\cos(\beta_0\tau/2)+\beta_1/\beta_0 \sin(\beta_0\tau/2)\} \quad (5)$$

where

$$\beta_0^2 = 4\omega_1^2-\beta_1^2 .$$

According to the Wiener-Khinchin-theorem, the spectral density is proportional to the Fourier transform of the autocorrelation function

$$J_\chi(\omega) = \mathfrak{F}\,\{\langle \chi(t)\,\chi(t+\tau)\rangle\} , \quad (6)$$

where $\mathfrak{F}$ denotes the Fourier transform. The spectral densities determined from the trajectories can therefore be compared to the Fourier transform of the analytic expression in Eq.(5)

$$\mathfrak{F}(\langle \Phi_i(t)\,\Phi_i(t+\tau)\rangle) = \langle \Phi_i^2(t)\rangle\, 2\beta_1\omega_1^2/\{(\omega^2-\omega_1^2)^2+\beta_1^2\omega_1^2\} , \quad (7)$$

a fitted curve of which is also included in Fig.3. Averaged damping coefficients β_1 for the main oscillation about the axis X' and Y' determined from the fittings are given in Table 1. To compare the MD simulations and the results of EPR experiments it is useful to calculate values of the fluctuation angles θ of the molecular z-axis (see Fig.1) rather than the reorientation of the nitroxide about a single axis, Φ. Values of $\langle \theta^2(t)\rangle^{1/2}$ including all frequencies are given in Table 1. These amplitudes range from 12° to 15° for the different model systems. The corresponding values for $\langle r^2(t)\rangle^{1/2}$ for the two C-atoms of the C−N−C group, e.g., are 0.014nm and 0.019nm for model system 3. These values are typical and consistent with results of MD simulations of other authors for atom fluctuations of protein side chains [12].

3. EPR Spectra Analysis

3.1. The Spin Hamiltonian

In the absence of motion the EPR spectra of nitroxide radicals with $S=1/2$ are adequately described by the Hamiltonian [25]

$$\mathfrak{H} = g_{zz}\beta_e B_0 S_z + A_{zz}S_zI_z + A_{xz}S_zI_z + A_{yz}S_zI_z \quad (8)$$

with the eigenvalues

$$E = g(\theta,\phi)\,\beta_e B_0 M_s + A(\theta,\phi)\,M_s M_I \quad (9)$$

where

$$g(\theta,\phi) = g_{xx}l_{zx} + g_{yy}l_{zy} + g_{zz}l_{zz} \quad (10)$$

and

Table 1
Comparison of parameters determined from molecular dynamic simulations and EPR experiments

System	Molecular dynamics simulation 1[1)]	2 (in vacuo)	3	4 ("solved")	EPR experiment JaaSl (lyophilized)	MalSl (lyophilized)	JaaSl (solved)	MalSl (solved)
$\langle\theta^2\rangle^{1/2}_{300\,K}$/deg	12	15	15	12	13	13	11	9
$\log(\omega_1/2\pi/s^{-1})$	11.9	11.9	11.7	12.2	>9	>9	12.7[2)]	11.3[2)]
$\log(\beta_1/s^{-1})$	12.0	11.9	11.5	12.4	–	–	–	–

[1)] The values are averages calculated from the results for the two spin labels attached to the β_1 and β_2 subunits of the methemoglobin tetramer.
[2)] Calculated from the intercept of the regression lines shown in Fig.6.

$$A(\theta,\phi) = \{A_{xx}^2 l_{zx} + A_{yy}^2 l_{zy} + A_{zz}^2 l_{zz}\}^{1/2} \tag{11}$$

g_{xx}, g_{yy}, g_{zz} and A_{xx}, A_{yy}, A_{zz} are the principle values of the g-tensor and hyperfine tensor, respectively. β_e is the electron Bohr magneton, B_0 the laboratory magnetic field vector, S the electron spin operator and I the N nuclear spin operator. M_s and M_I denote the electron and nuclear spin quantum numbers, respectively. The parameters l_{ij} depend on the orientation of the nitroxide molecule with respect to the laboratory frame and are given in spherical coordinates by

$$l_{zx} = (-\sin\theta\cos\varphi)^2,\ l_{zy} = (\sin\theta\sin\varphi)^2, \text{ and } l_{zz} = (\cos\theta)^2 . \tag{12}$$

3.2. Rapid Reorientational Motion

Introducing rapid reorientational motion, Eq.(8) becomes

$$\mathcal{H} = \langle g_{zz}\rangle \beta_e B_0 S_z + \langle A_{zz}\rangle S_z I_z + \langle A_{xz}\rangle S_z I_z + \langle A_{yz}\rangle S_z I_z \tag{13}$$

where the angular brackets indicate spatial averaging resulting from the reorientational fluctuations of the nitroxide axes with respect to the stationary laboratory magnetic field. This approximation is valid if the motion is fast compared to the EPR time scale which is defined by the anisotropy of the g- and A-tensors: e.g. $\hbar\,|A_{zz}-A_{xx}|^{-1} \approx 10^{-9}$ s. Van and coworkers [26] have shown for different motional mechanisms that the simple Eqs. (10–12) are retained if the principle values g_{ii} and A_{ii} are replaced by their spatial averaged counterparts.

3.3. Coordinate Transformation

Eqs. (9–12) are written in terms of one matrix L that rotates the nitroxide xyz axes into the laboratory XYZ axis system. Again we introduce one more intermediate coordinate system $X'Y'Z'$ in which we perform the spatial averaging (see Fig.1). The transformation matrices L' and L_0, which are defined in terms of the three Eulerian angles, θ,φ,ψ, rotate the nitoxide coordinate system xyz into the sample system $X'Y'Z'$ and successively into the laboratory coordinate system, according to Fig.2 of Ref. [26]:

$$\begin{pmatrix} X \\ Y \\ Z \end{pmatrix} = L_0 \begin{pmatrix} X' \\ Y' \\ Z' \end{pmatrix} = L_0 L' \begin{pmatrix} x \\ y \\ z \end{pmatrix}. \tag{14}$$

From the results of our molecular dynamics simulations we expect that the molecular axes xyz of the spin label execute a rapid random walk over part of the surface of a sphere in the coordinate system $X'Y'Z'$ (cf. Figs. 1 and 2). The spatial averaged values of the hyperfine tensor $A_{X'Y'Z'}$ in the sample coordinate system are calculated according to

$$\langle A_{X'Y'Z'}\rangle = \langle L'^{\tau} A_{xyz} L'\rangle \tag{15}$$

where τ indicates transpose. In practice the hyperfine tensor of the used spin labels are very nearly axially symmetric and it is a good approximation to set $A_{xx} = A_{yy} = A_\perp$ and a rotation about the z-axis with angle ψ needs not to be specified. Consequently we define $A_{zz} = A_\parallel$. The matrix elements of $A_{X'Y'Z'}$ contain products of the direction cosines $\langle\cos^2\theta\cos^2\varphi\rangle$. It is useful to perform a simplification: We assume that the nitroxide molecular z-axis points with equal probability in all directions with respect to the angle φ. Then $\langle\cos^2\varphi\rangle$ becomes 0.5. This assumption is justified by the results of the molecular dynamics simulations: from the trajectories we get $\langle\cos^2\varphi\rangle$ = 0.44, 0.6, 0.47, and 0.49 for systems 1 through 4. In this case Eq.(15) reads simply

$$\langle A_{X'Y'Z'}\rangle = \begin{pmatrix} \bar{A}_\perp & 0 & 0 \\ 0 & \bar{A}_\perp & 0 \\ 0 & 0 & \bar{A}_\parallel \end{pmatrix} \tag{16}$$

where

$$\bar{A}_\parallel = A_\perp + (A_\parallel - A_\perp)\langle\cos^2\theta\rangle$$
$$\bar{A}_\perp = A_\perp + (A_\parallel - A_\perp)(1-\langle\cos^2\theta\rangle)/2 . \tag{17}$$

For small amplitude fluctuations $\langle\theta^2\rangle$ these equations reduce to

$$\bar{A}_\parallel = A_\parallel + (A_\perp - A_\parallel)\langle\theta^2\rangle$$
$$\bar{A}_\perp = A_\perp + (A_\parallel - A_\perp)\langle\theta^2\rangle/2 . \tag{18}$$

Replacing $\langle\theta^2\rangle$ by the solution of the Langevin equation, Eq.(2), $\langle\theta^2\rangle = 2kTl/(I\omega^2)$, we conclude that the averaged tensor elements should show a linear behavior with temperature.

3.4. Reorientational Fluctuations of the Nitroxide Ring in a Stable Conformational Substate: Determination of $\langle\theta^2\rangle_{exp}$ and Comparison with $\langle\theta^2\rangle_{sim}$

In the following section the motional averaged values of the hyperfine tensor of two different spin labels attached to methemoglobin are determined from the experimental EPR spectra and the results are discussed in relation to the model of the Brownian oscillator. The experimentally determined values of the magnitude of the nitroxide ring fluctuations are compared to the values calculated from the MD simulations.

Replacing A_{xx}, A_{yy} in Eq.(11) by $\bar{A}_\perp$ of Eq.(18) and A_{zz} by $\bar{A}_\parallel$ the transformation from the sample system into the laboratory coordinate system is performed by the parameters l_{IJ}, Eq.(12), where the angles θ and φ are now the Eulerian angles between the sample coordinate system and the laboratory system. By using Eq.(9) the motional averaged ESR spectra are calculated. Least squares fitting of the calculated spectra to experimental ESR spectra yields the parameters $\bar{A}_\parallel$ and $\bar{A}_\perp$. The fitting procedure as well as the materials and equipment used are described in detail in Refs. [8,9]. Additionally to the spin label JaaSl used in the MD simulations a further label is applied in the EPR experiments: 4-maleimido-2,2,6,6-tetramethyl-piperidinyl-1-oxyl(MalSl). This label attached to cystein β93 of hemoglobin occupies the tyrosin pocket corresponding to state A for JaaSl [20]. To ensure unique results and high resolution nitroxide spin labels with ^{14}N and ^{15}N isotopes are used [10,27]. The results of $\bar{A}_\parallel$ determined from least squares fittings to spectra of the lyophilized dry samples are shown in Fig.4a. For the solved samples the averaging parameter

$$S = \frac{\bar{A}_\parallel - 1/3\ \mathrm{Tr}\ A}{A_\parallel - 1/3\ \mathrm{Tr}\ A} \qquad (19)$$

is used rather than $A_\parallel$. Tr A is the trace of the hyperfine tensor. S changes from 1 for the rigid limit value, $\bar{A}_\parallel = A_\parallel$, to zero in the case of complete averaging, $\bar{A}_\parallel = 1/3$ Tr A. The choice of S as a measure of the motional averaging of the spectra allows for the comparison of spin labels with different values of the hyperfine tensor due to different configurations of the label or different polarities of the label environment. The behavior of S with temperature of the methemoglobin samples in solution is given in Fig.4b. The measured values of $\bar{A}_\parallel$ decrease linearly with increasing temperature up to 320K for the lyophilized systems and up to about 220K for the water containing samples. This behavior is consistent with the observations of Johnson [28], results of our previous measurements [8,9] and the predictions of our simple model, Eq.(18). The traces of the hyperfine tensors of all samples are shown in Fig.4c and are found to be constant within experimental error in the whole

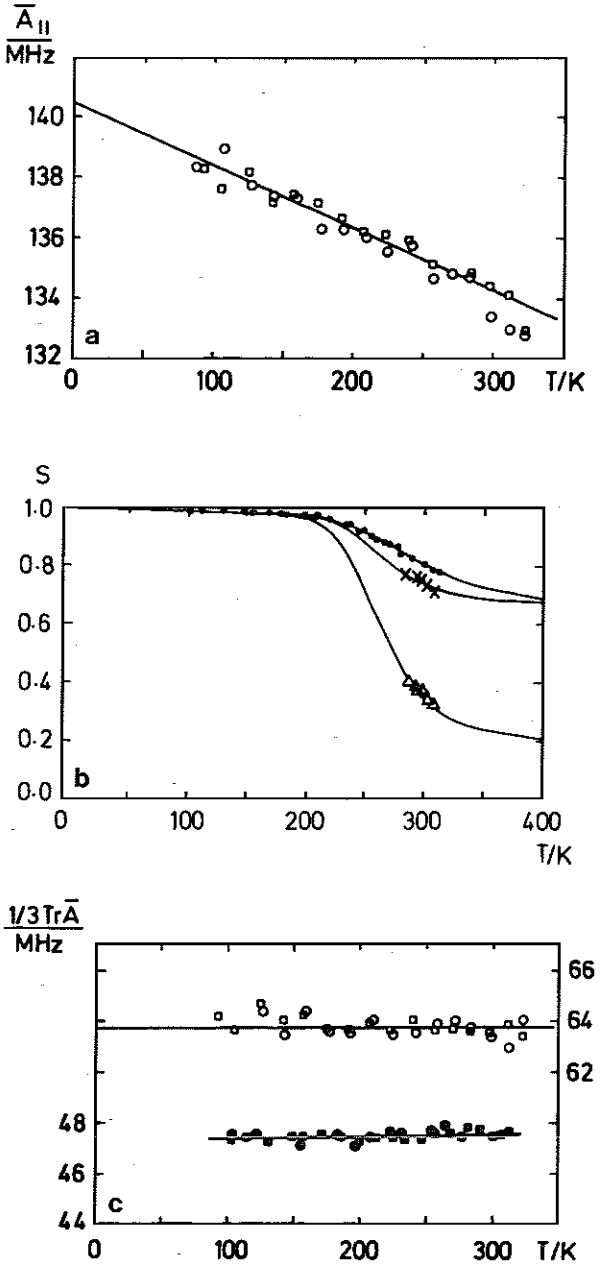

Fig. 4
a) The motional averaged hyperfine tensor element $\bar{A}_\parallel$ of lyophilized dry spin labelled methemoglobin samples as a function of temperature: (□), methb-^{15}N-MalSl; (○), methb-^{15}N-JaaSl.
b) The behavior of the averaging parameter S with temperature for solved spin labelled methemoglobin: (●), methb-^{14}N-MalSl; (×), methb-^{15}N-JaaSl with S determined from spectral parameters corresponding to state A; (△), methb-^{15}N-JaaSl with S determined from spectral parameters corresponding to state B. The lines are fits of $S(\theta,r)$ according to Eq.(21) to the experimental data points.
c) 1/3 trace A for spin labelled methemoglobin as a function of temperature. Lyophilized dry samples: (○), methb-^{15}N-JaaSl; (□), methb-^{15}N-MalSl. Samples in solution: (●), methb-^{14}N-JaaSl; (■), methb-^{14}N-MalSl

temperature range investigated. Therefore the changes of $\langle A_{XYZ}\rangle$ due to temperature induced polarity changes of the environment of the spin label binding site are negligible small. From the slope of the regression lines to the exper-

imental data points between 80 and 320K for the dry samples and between 80 and 220K for the solved samples the values of $\langle\theta^2(T = 300\text{K})\rangle^{1/2}$ are calculated according to Eq.(18) and given in Table 1. For the methb-JaaSl samples these values are an average of state A and B because the respective parts cannot be separated from the EPR spectra. A comparison with the results determined from the methb-MalSl samples, where the spin label occupies the tyrosin pocket according to state A of the methb-JaaSl sample, indicates that the difference in magnitude of the harmonic fluctuations in both states should be negligible at least for the lyophilized samples. In the presence of a hydration sphere the magnitude of the oscillations is reduced. This is a consequence of the interaction of the water molecules with the fluctuating side chain which acts in the sence of an enhanced curvature of the potential hole. This behavior as well as the magnitudes of the oscillations are in good agreement with the results of the molecular dynamics simulations. We conclude that the model of a Brownian particle bound within a harmonic potential and in contact with a heat bath is a good description for the motional behavior of the nitroxide group within the temperature range discussed above. The sigmoidal behavior of S of the solved samples for temperatures above 200K, however, cannot be explained by a harmonic reorientation of the nitroxide ring and we will extend our model in the next section.

3.5. Slow Reorientational Motion: Transitions between Conformational Substates. Estimation of $\omega_{1,\text{exp}}$ and Comparison with $\omega_{1,\text{sim}}$

For temperatures above 200K the behavior of S with temperature changes drastically for the solved protein samples compared to the linear behavior of $\bar{A}_\parallel$ below 200K (see Fig.4b). The degree of motional narrowing determined from the spectra depends on the spin label used and the conformation of the modified protein (state A or B) and is largest for methb-JaaSl in state B. The underlying processes will be explained by transitions between conformational substates of the modified protein corresponding to local minima of the potential energy within state A and B with rates r_A and r_B as shown in Fig.5 (see also [8]). The sequence of transitions between conformational substates which are setting in above 200K in consistency with results of flash photolyse experiments on the rebinding reactions of CO in myoglobin [29] are reflected in our EPR experiment by the residual reorientation of the nitroxide ring of the spin label with respect to the whole protein molecule.

To account for this fluctuation process and the concerning changes of the EPR spectra a simple two state jump model is applied which is to allow the molecular z-axis of the nitroxide ring to jump between two orientations characterized by the semiangle θ of the limited motion cone with rate r

$$r = r^* \exp(-E_a/kT) \,. \tag{20}$$

E_a is the height of the potential barrier between the two

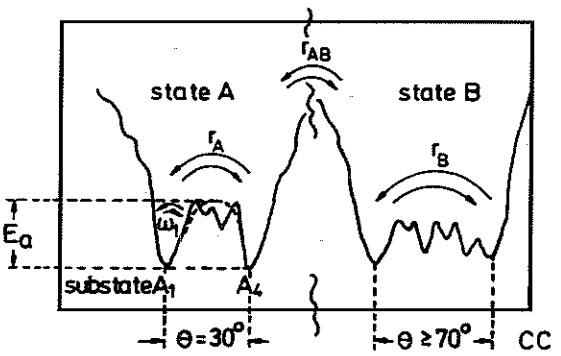

Fig. 5
A one dimensional cross section through the multidimensional conformational energy landscape of methemoglobin is sketched as a function of the conformational coordinate CC. States A and B correspond to the different conformations discussed in section 2. Transitions within state A are possible between substates marked with arbitrarily chosen subscripts 1 and 4 by an escape over the potential barrier (dashed line) of height E_a with rate r_A. The ranges of the conformational space coated by the reorientational motion of the nitroxide ring within state A and B are characterized in terms of a two jump model by two different values of the jump angle θ

states. There is evidence in our molecular dynamics simulations that the approach of a two state jump model for the nitroxide ring fluctuations within a given conformational state may be justified. From the trajectory of model system 3 (state B) shown in Fig.2a we recognize two conformational transitions with a sudden changes of ϕ of about 70°. The fluctuation process is not fast compared to the EPR time scale and Eq.(13) is no more valid in this case. Instead the EPR spectra have to be calculated solving the stochastic Liouville equation [30] with a time dependent Hamiltonian. Spectral simulations for the two state jump model with different values of the jumping rate r and semi angle θ have been performed [8]. From an effective averaging of the tensor elements of the hyperfine tensor according to Eq.(19) or the shift of the low field peak with respect to the magnetic B_0 field axis the averaging parameter $S(\theta,r)$ is extracted from the simulated spectra. Calibration curves for S vs. r for different values of θ are calculated in this way and an empirical expression for the behavior of S yields

$$S(\theta,r) = \frac{S(\theta,r\to\infty) + (6ar)^{-1/b}}{1 + (6ar)^{-1/b}} \tag{21}$$

with $a = 2.3 \cdot 10^{-9}$s, $b=0.87$ and the values of $S(\theta,r\to\infty)$ being given in Fig.2 of Ref.[9]. Least squares fittings of $S(\theta,r)$, Eq.(21), with r given by Eq.(20) to the temperature dependent values $S(T)$, which are determined from the experimental spectra, yield values of $S(\theta,r\to\infty)$ and therefore of the semi angle θ, the frequency factor r^*, and the height of the energy barrier E_a. The values of θ are found to be temperature independent in the temperature range investigated [9].

For temperatures above 280K the low field peaks of the spectra of JaaSl spin labelled methemoglobin in conformational state A and B can clearly be distinguished and

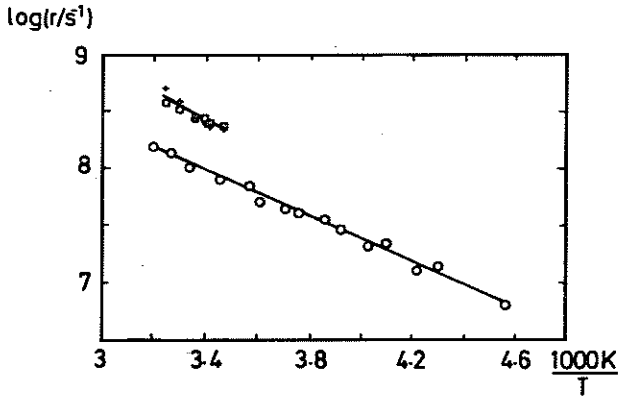

Fig. 6
Arrheniusplot of the reorientational motion of the nitroxide within state A and B. (○), methb-^{14}N-MalSl, state A; (+), methb-^{15}N-JaaSl, state A; (□), methb-^{15}N-JaaSl, state B

application of the method described above yields values of θ of 30°±2° and ≥70° for the reorientational fluctuation of the nitroxide group within state A and state B, respectively (see Fig.4b). The behavior of S of methb-MalSl with temperature is similar to that of methb-JaaSl in state A. The best fit of Eq.(21) to the experimental data points yields a corresponding semi angle θ of the limited motion cone of 30°±2°. Using the respective values of $S(\theta, r\to\infty)$ the rates r are calculated from the experimental values $S(T)$ by means of Eq.(21). These values are shown in an Arrhenius plot, Fig.6, for methb-JaaSl for states A and B and for methb-MalSl. Despite of different angles of fluctuation of the nitroxide group of JaaSl within the two conformational states A and B the rates appear to coincide within experimental error, averaged values of r^* for both states being given in Table 1. The rates of the reorientation of MalSl are slightly less compared to the results of the JaaSl label. This may be a consequence of a minor flexibility of the structure of MalSl which connects the cystein side chain with the nitroxide ring. All curves show linear behavior which we attribute to the relatively small temperature range investigated since it is known from investigations of the flash photolysis experiments [31] that relaxation processes in proteins are non-Arrhenius in temperature. We take the Arrhenius model as a first approach and calculate the values of the activation energy E_a and the frequency factor r^* from the slopes and intercepts of the regression lines. For methb-JaaSl in state A and B the values of E_a coincide within experimental error, E_a = (24±3) kJ/mol, for methb-MalSl we get (19±1) kJ/mol. The values of r^* are shown in Table 1. The behavior of S with temperature for the two states A and B can adequately be explained by transitions between conformational substates within the respective states. Transitions between states A and B seem to have no influence on the EPR spectra and the corresponding transition rate r_{AB} shown in Fig.5 should therefore be less than 10^7 s^{-1}.

To bridge our short time molecular dynamics simulation and the long time transitional dynamics observed in our experiments we extend our model of the Brownian oscillator: We make use of Kramers' derivation of the Fokker-Planck equation which accounts for the rates at which particles that are initially caught in a potential hole will escape over the potential barrier of hight E_a in consequence of Brownian motion. The parameters relevant for this model are explained in Fig.5 in terms of our experimental results. The rate of escape is given in an one-dimensional treatment by [24]

$$r = \frac{\omega_1\beta_1}{4\pi}\left\{\left(1+\frac{4\omega_2^2}{\beta_1^2}\right)^{1/2}-1\right\}\exp(-E_a/kT) \tag{22}$$

where ω_2 is a measure of the curvature of the energy function at the top of the barrier. If $\beta_1 \ll \omega_1$, which is the case for the fluctating nitroxide ring (c.f. Table 1), Eq.(22) reduces to

$$r = \omega_1/(2\pi)\exp(-E_a/kT) \tag{23}$$

and r^* in Eq.(20) corresponds to $\omega_1/(2\pi)$ in Eq.(23). The molecular dynamics simulation show that the oscillation of the nitroxide ring about the molecular x- and y-axes are of similar amplitude and frequency. So we take the one-dimensional treatment of the problem as a first approximation and compare the values of r^* determined from the EPR-experiments and values of $\omega_1/(2\pi)$ calculated from the molecular dynamic simulation in Table 1. Again good agreement is achieved between the experimental and the simulated values.

The results of our MD simulations give indications of the amplitude of the nitroxide reorientation. The twofold change of ϕ of 70°−100° present in the trajectory of ϕ_1 of methb-JaaSl in state B (see Fig.2) shows that large scale reorientations of the nitroxide ring about the X' axis are not unlikely. The experiment yields a comparable value of the semi angle of the limited motion cone of 70° on the basis of the two state jump model. The trajectory, however, is to short to make any statistics. MD simulations with trajectories which are much longer or alternative methods as Brownian dynamics simulations or activated dynamics simulations [12] could be helpful in this case to join theoretical and experimental methods concerning the dynamics of protein side chains.

4. Conclusions

The present paper combines MD simulations and EPR data to enhance the understanding of internal motions in proteins. The effects on EPR parameters of rapid small scale motions within a given potential well observed in MD simulations can be calculated. The determined EPR data are consistent with the magnitude and frequency of such motions predicted by the simulations. The rates of the relatively large fluctuations involving rare jumps between different potential wells cannot be predicted from short time simulations. Much longer simulations or alternative approaches are needed here to account for the experimental results. Nevertheless, it is possible by use of a simple model to compare the experimentally determined frequency factor

for the transitions between conformational substates and the oscillation frequency of the fluctuations within a single substate.

We conclude that EPR studies can serve as a test of many aspects of molecular dynamics simulations and that simulations can enhance the interpretation of EPR experiments. Recent advances in molecular genetics have made it possible to introduce spin labels at arbitrarily chosen sites within proteins using site-directed mutagenesis [32]. The analysis of the attached spin labels by EPR spectroscopy in combination with computer simulation techniques will enhance the understanding of protein dynamics and rate processes in systems of similar complexity.

We would like to thank J. Schlitter and Prof. A. Redhardt for helpful discussions, and Silicon Graphics, Köln, and Biosym, München, for the disposition of computer hardware and software.

References

[1] R. H. Austin, K. W. Beeson, L. Eisenstein, H. Frauenfelder, and I. C. Gunsalus, Biochemistry *14*, 5355 (1975).
[2] H. Frauenfelder, F. Parak, and R. D. Young, Annu. Rev. Biophys. Biophys. Chem. *17*, 451 (1988).
[3] R. Elber and M. Karplus, Science *235*, 318 (1987).
[4] M. K. Hong, D. Braunstein, B. R. Cowen, H. Frauenfelder, I. E. T. Iben, J. R. Mourant, P. Ormos, R. Scholl, A. Schulte, P. J. Steinbach, A.-H. Xie, and R. D. Young, Biophys. J. *58*, 429 (1990).
[5] L. J. Berliner, Spin Labeling I, Theory and Application, Academic Press Inc., New York 1976.
[6] L. J. Berliner, Spin Labeling II, Academic Press Inc., New York 1979.
[7] L. J. Berliner and J. Reuben, Biological Magnetic Resonance 8, Spin Labeling, Plenum Press, New York 1989.
[8] H. J. Steinhoff, K. Lieutenant, and J. Schlitter, Z. Naturforsch. *44c*, 280 (1989).
[9] H. J. Steinhoff, Eur. Biophys. J. *18*, 57 (1990).
[10] H. J. Steinhoff, O. Dombrowsky, C. Karim, and C. Schneiderhan, Eur. Biophys. J. *20*, 293 (1991).
[11] M. Karplus, in: Methods in Enzymology 131, eds. C. H. Hirs and S. N. Timasheff, Academic, New York 1986.
[12] J. A. McCammon and S. C. Harvey, Dynamics of proteins and nucleic acids, Cambridge University Press, Cambridge 1987.
[13] H. Frauenfelder, G. A. Petsko, and D. Tsernoglou, Nature *280*, 558 (1979).
[14] S. H. Northrup, M. R. Pear, J. A. McCammon, M. Karplus, and T. Takano, Nature *287*, 659 (1980).
[15] W. F. van Gunsteren and M. Karplus, Nature *293*, 677 (1981).
[16] G. Lipari and A. Szabo, J. Am. Chem. Soc. *104*, 4546 (1982).
[17] C. M. Dobson and M. Karplus, in: Methods in Enzymology 131, eds. C. H. Hirs and S. N. Timasheff, pp. 362, Academic, New York 1986.
[18] R. C. Ladner, E. J. Heidner, and M. F. Perutz, J. Mol. Biol. *114*, 385 (1977).
[19] J. Lajzerowicz-Bonneteau, in: Spin Labeling Theory and Applications, ed. L. J. Berliner, pp. 239, Academic Press, New York 1976.
[20] J. F. Moffat, J. Mol. Biol. *55*, 135 (1971).
[21] H. M. McConnell and C. Hamilton, Proc. Nat. Acad. Sci. *60*, 776 (1968).
[22] C. L. Brooks and M. Karplus, J. Mol. Biol. *208*, 159 (1989).
[23] P. Ahlström, O. Teleman, B. Jönsson, and S. Forsen, J. Ann. Chem. Soc. *109*, 1541 (1987).
[24] S. Chandrasekhar, Rev. Mod. Phys. *15*, 1 (1943); G. E. Uhlenbeck and L. S. Ornstein, Phys. Rev. *36*, 823 (1930); C. W. Ming and G. E. Uhlenbeck, Rev. Mod. Phys. *17*, 323 (1945).
[25] L. J. Libertini and O. H. Griffith, J. Chem. Phys. *53*, 1359 (1970).
[26] S. P. Van, G. B. Birrell, and O. H. Griffith, J. Magn. Reson. *15*, 444 (1974).
[27] B. J. Gaffney, C. H. Elbrecht, and J. P. A. Scibilia, J. Magn. Reson. *44*, 436 (1981).
[28] M. E. Johnson, Biochemistry *17*, 1223 (1978).
[29] H. Frauenfelder, G. U. Nienhaus, and J. B. Johnson, Ber. Bunsenges. Phys. Chem. *95*, 272 (1991).
[30] D. J. Schneider and J. H. Freed, in: Biological Magnetic Resonance 8, Spin Labeling, ed. L. J. Berliner and J. Reuben, pp. 1, Plenum Press, New York 1989.
[31] R. D. Young, H. Frauenfelder, J. B. Johnson, D. C. Lamb, G. U. Nienhaus, R. Philipp, and R. Scholl, Chem. Phys. *158*, 315 (1991).
[32] C. Altenbach, T. Marti, H. G. Khorana, and W. L. Hubbell, Science *248*, 1088 (1990).

(Received: September 22th, 1992) E 8148